

# 1 Improvement of the KarstMod modeling 2 platform for a better assessment of karst 3 groundwater resources

4 Vianney Sivellev<sup>1</sup>, Guillaume Cinkus<sup>1,2</sup>, Naomi Mazzilli<sup>2</sup>, David Labat<sup>3</sup>, Bruno Arfib<sup>4</sup>, Nicolas Massei<sup>5</sup>,  
5 Yohann Cousquer<sup>1</sup>, Dominique Bertin<sup>6</sup> and Hervé Jourde<sup>1</sup>

6  
7 <sup>1</sup> HSM, Univ Montpellier, CNRS, IRD, Montpellier, France

8 <sup>2</sup> EMMAH, INRAE, Avignon Université, 84000 Avignon, France

9 <sup>3</sup> Géosciences Environnement Toulouse UMR CNRS IRD Université Paul Sabatier CNES, 14 Avenue  
10 Edouard Belin 31400, Toulouse

11 <sup>4</sup> Aix-Marseille Univ, CNRS, IRD, INRAE, Coll de France, CEREGE, Aix-en-Provence, France

12 <sup>5</sup> Univ Rouen Normandie, Univ Caen Normandie, CNRS, M2C, UMR 6143, F-76000 Rouen, France

13 <sup>6</sup> GEONOSIS, France

14 Correspondence: vianney.sivelle@umontpellier.fr

## 15 Abstract

16 Hydrological models are fundamental tools for the characterization and management of karst systems.  
17 We propose an updated version of KarstMod, [software](#) dedicated to lumped parameter rainfall-discharge  
18 modeling of karst aquifers. KarstMod provides a modular, user-friendly modeling environment for  
19 educational, research, and operational purposes. It also includes numerical tools for time series analysis,  
20 model evaluation, and sensitivity analysis. The modularity of the platform facilitates common operations  
21 related to lumped parameter rainfall-discharge modeling, such as (i) setup and parameter estimation of  
22 a relevant model structure, and (ii) evaluation of internal consistency, parameter sensitivity, and  
23 hydrograph characteristics. The updated version now includes (i) external routines to better consider the  
24 input data and their related uncertainties, i.e. evapotranspiration and solid precipitation, (ii) enlargement  
25 of multi-objective calibration possibilities, allowing more flexibility in terms of objective functions as  
26 well as observation type and (iii) additional tools for model performance evaluation including further  
27 performance criteria and tools for model errors representation.

## 28 1 Introduction

29 Karst aquifers constitute an essential source of drinking water for about 9.2% of the world population  
30 (Stevanović, 2019) and it is estimated that one-quarter of the world population depends on freshwater  
31 from karst aquifers (Ford and Williams, 2013). Karst aquifers contain an important volume of freshwater

32 while only 1% of its annually renewable water is used for drinking water supply (Stevanović, 2019).  
33 Understanding the functioning of karst aquifers and developing operational tools to predict the evolution  
34 of freshwater resources is therefore a major challenge for the hydrological science community (Blöschl  
35 et al., 2019). To this day, the number of tools dedicated to karst hydrogeology is limited and is mostly  
36 developed for academic purposes and not user-friendly. Nonetheless, such tools are required for a better  
37 assessment of groundwater vulnerability as well as sustainable management of the groundwater  
38 resources (Elshall et al., 2020) and should be handled by the stakeholders without programming skills  
39 requirements.

40 KarstMod is an adjustable modeling platform (Mazzilli et al., 2019) dedicated to lumped parameter  
41 rainfall-discharge modeling allowing for (i) simulation of spring discharge, piezometric head and  
42 surface water discharge (Bailly-Comte et al., 2010; Cousquer and Jourde, 2022; Sophocleous, 2002),  
43 (ii) analysis of the internal fluxes considered in the model, (iii) model performance evaluation and  
44 parametric sensitivity analysis. In this paper, we present the new features incorporated in KarstMod: (i)  
45 external routines to better consider the input data and their related uncertainties, i.e. evapotranspiration  
46 and solid precipitation, (ii) enlargement of multi-objective calibration possibilities, allowing more  
47 flexibility in terms of objective functions as well as observation type with the possibility to include  
48 surface water discharge in the calibration procedure and (iii) model performance evaluation, including  
49 additional performance criteria as well as additional tools for model errors representation such as the  
50 diagnostic efficiency plot (Schwemmler et al., 2021). Also, we present two case studies to illustrate how  
51 KarstMod is useful in the framework of the assessment of karst groundwater resources and its sensitivity  
52 to groundwater abstraction. Section 2 is devoted to the presentation of the background and motivations  
53 to improve the functionalities of the platform while Sect. 3 presents the [key features](#) of KarstMod.  
54 Section 4 illustrates the application of rainfall-discharge modeling using KarstMod within the Touvre  
55 (western France) and the Lez (southern France) karst systems, which both constitute strategic freshwater  
56 resources and ensure drinking water supply.

## 57 **2 Background and motivations**

### 58 **2.1 Challenges in karst groundwater resources**

59 Karst aquifers are affected by the combination of different components of global change such as (i)  
60 effects of climate change which are particularly pronounced in the Mediterranean area (Dubois et al.,  
61 2020; Nerantzaki and Nikolaidis, 2020), (ii) increasing groundwater abstraction (Labat et al., 2022), as  
62 well as (iii) changes in land cover land use (Bittner et al., 2018; Sarrazin et al., 2018). Therefore, the  
63 assessment of karst groundwater resources sensitivity, in terms of quantity, requires operational tools  
64 for estimating the sustainable yield of karst aquifers but also to predict the impacts of climatic or  
65 anthropogenic forcing on groundwater resources in the long term (Sivelle et al., 2021). To address these  
66 issues, different modeling approaches have been developed (Jeannin et al., 2021) such as, among others,

67 fully-distributed models (Chen and Goldscheider, 2014), semi-distributed models (Doummar et al.,  
68 2012; Dubois et al., 2020; Ollivier et al., 2020), and lumped parameter models (Mazzilli et al., 2019)  
69 including semi-distributed recharge (Bittner et al., 2018; Sivelles et al., 2022b). Among these, lumped  
70 parameter models are recognized as major tools to explore the ability of conceptual representations to  
71 explain observations in karst systems (Duran et al., 2020; Frank et al., 2021; Poulain et al., 2018; Sivelles  
72 et al., 2019) and for managing karst groundwater resources (Cousquer and Jourde, 2022; Labat et al.,  
73 2022; Sivelles et al., 2021; Sivelles and Jourde, 2020).

## 74 **2.2 Challenges in lumped parameters modeling in karst hydrology**

75 Lumped parameter models consist of a functional approach that analyzes a hydrogeological system at  
76 the catchment scale and describes the transformation from rainfall into discharge using empirical or  
77 conceptual relationships. Therefore, parameter values or distributions cannot be determined directly  
78 from catchment physical characteristics or in-situ measurements, except the discharge coefficient to the  
79 spring that can be estimated based on recession curve analysis. Instead, model parameter values must  
80 be estimated by history-matching. In a general way, rainfall-discharge models in karst hydrology are  
81 calibrated considering spring discharge measurements. Former studies have shown an interest in  
82 considering hydrochemical observations (Chang et al., 2021; Hartmann et al., 2013; Sivelles et al., 2022a)  
83 but such an approach requires further methodological development before being included in KarstMod.  
84 To date, KarstMod allows considering complementary observations only with piezometric head and  
85 surface water discharge (Cousquer and Jourde, 2022).

86 Another challenge concerns the evaluation of the water fluxes within the soil-vegetation-atmosphere  
87 continuum. Bittner et al. (2021) computed several models to evaluate the fluxes related to interception,  
88 evapotranspiration, and snow process. The results show significant uncertainties related to input data as  
89 well as potential compensation between the various uncertain processes. In some cases, snow melt is a  
90 controlling factor in the water balance (Doummar et al., 2018; Liu et al., 2021), thus a suitable snowmelt  
91 estimation is required to improve hydrological model performance (Çallı et al., 2022). Therefore, two  
92 meteorological modules have been added to KarstMod: (i) a "Snow routine" and (ii) a routine to compute  
93 the potential evapotranspiration  $PET$  ( $\text{mm day}^{-1}$ ), denoted "PET routine". The two additional modules  
94 allow us to better account for snow and evapotranspiration processes.

## 95 **3 Implementation**

96 The updated version of KarstMod implements additional features to enhance the rainfall-discharge  
97 modeling practices. First, we describe the additional modules (snow and PET routines) for a better  
98 meteorological forcing estimation. Then, we introduce the additional tools proposed for (i) the setup and  
99 calibration of the model structure, (ii) model performance evaluation as well as (iii) uncertainties  
100 consideration. Fig. 1 shows a screenshot of the KarstMod software.

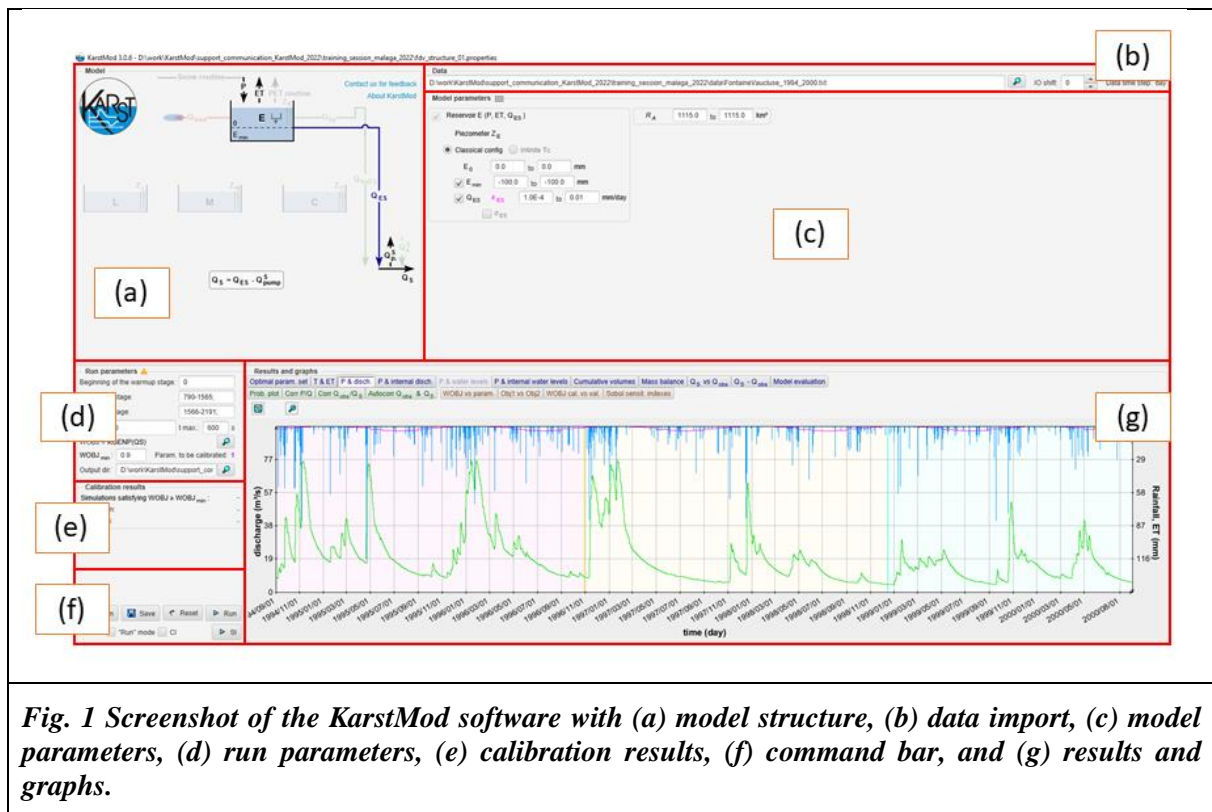


**Fig. 1** Screenshot of the KarstMod software with (a) model structure, (b) data import, (c) model parameters, (d) run parameters, (e) calibration results, (f) command bar, and (g) results and graphs.

### 101 3.1 Meteorological modules

#### 102 3.1.1 Snow routine

103 KarstMod allows using either observation-based precipitation time series  $P$  ( $\text{mm day}^{-1}$ ) or estimated  
 104 precipitation time series  $P_{Sr}$  ( $\text{mm day}^{-1}$ ) using a snow routine. The latter is similar to the one used by  
 105 Chen et al. (2018) – without the radiation components – which has been successfully used for improving  
 106 the simulation of karst spring discharge in snow-covered karst systems (Chen et al., 2018; Cinkus et al.,  
 107 2023a). It consists of a modified HBV-snow routine (Bergström, 1992) for simulating snow  
 108 accumulation and melt over different sub-catchments based on altitude ranges ([appendix A](#)). Each sub-  
 109 catchment is defined by two values that the user must input: (i) the proportion among the whole  
 110 catchment (sum must be equal to 1) and (ii) the temperature shift, related to the altitude gradient. The  
 111 different estimated precipitation  $P_{Sr}^*$  ( $\text{mm day}^{-1}$ ) associated with the subcatchments are calculated and  
 112 summed to produce the estimated precipitation time series  $P_{Sr}$ , which corresponds to a single variable  
 113 representative of the catchment.  $P_{Sr}$  thus gives the water leaving the snow routine and is equivalent to  
 114 the recharge into the first compartment of the model (compartment E in KarstMod). The snow routine  
 115 workflow requires both air temperature  $T$  ( $^{\circ}\text{C}$ ) and precipitation  $P$  ( $\text{mm day}^{-1}$ ) time series.  $P$  is  
 116 considered as snow when  $T$  in the sub-catchment is lower than the temperature threshold  $T_s$  ( $^{\circ}\text{C}$ ). Snow  
 117 melts when the temperature exceeds the threshold according to a degree-day expression. The snow melt  
 118 is a function of the melt coefficient  $MF$  ( $\text{mm } ^{\circ}\text{C}^{-1} \text{ day}^{-1}$ ), and the degrees above the temperature  
 119 threshold. Runoff starts when the water level exceeds the liquid water holding capacity of snow  $CWH$

120 (-). The refreezing coefficient  $CFR$  (-) stands for refreezing liquid water in the snow when snow melt is  
 121 interrupted (Bergström, 1992). The output of the snow routine consists of a redistributed precipitation  
 122 time series  $P_{sr}$ . The four parameters of the snow routine (i.e.,  $T_s$ ,  $MF$ ,  $CWH$ , and  $CFR$ ) can be  
 123 considered in the parameter estimation procedure as well as sensitivity analysis. The snow routine  
 124 features can be activated from the model structure area (Fig. 1 a). Fig. 2 shows the general workflow  
 125 implemented in the snow routine.  $P_{sr}^*$  is estimated for each time step  $t$  based on the precipitation  $P$  and  
 126 air temperature  $T$  time series for each sub-catchment  $i$ . The total snow routine output  $P_{sr}$  is calculated  
 127 as a weighted sum of  $P_{sr}^*$  time series:

$P_{sr} = \sum_i^N P_{sr_i}^* \times p_i$	<u>Eq. 1</u>
---	--------------

128 where  $p_i$  is the proportion of the sub-catchment  $i$  regarding the complete catchment area such as  $\sum p_i =$   
 129  $1$ , and  $N$  is total number of sub-catchments. The snow routine allows estimating  $P_{sr}^*$  according to the  
 130 algorithm A1.

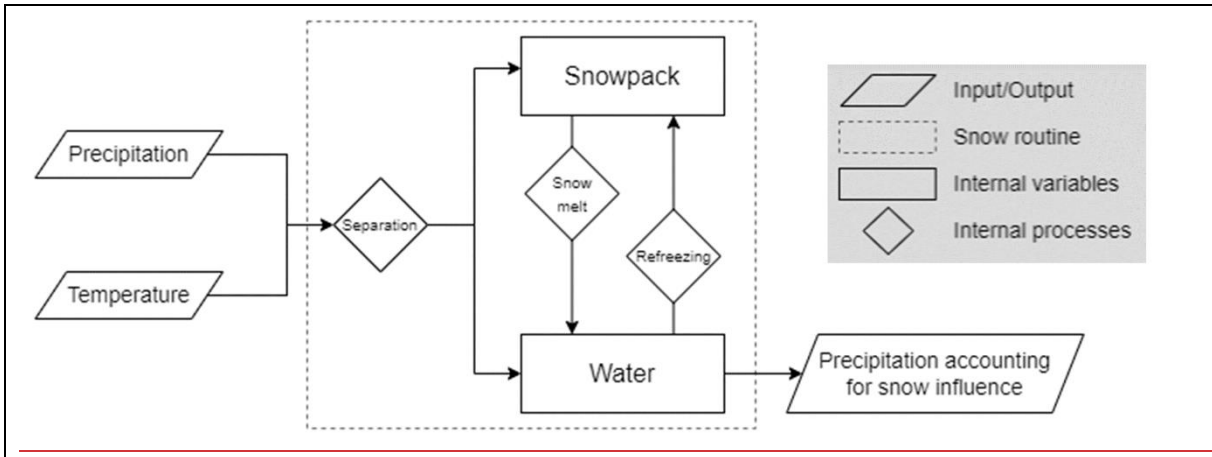


Fig. 2 Snow routine workflow.

131

**Algorithm A1** Estimating  $P_{sr}^*$  in sub-catchment

With  $P_{sr}^*$  = water leaving the routine/recharge to the soil ( $\text{mm day}^{-1}$ ),  $T_a$  = active temperature for snowmelt ( $^{\circ}\text{C}$ ),  $T_n$  = active temperature for refreezing ( $^{\circ}\text{C}$ ),  $m$  = snow melt ( $\text{mm day}^{-1}$ ),  $rfz$  = refreezing ( $\text{mm day}^{-1}$ ),  $v$  = solid component of snowpack depth (mm),  $vl$  = liquid component of snowpack depth (mm), and  $dt$  = temporal resolution.

**for  $t$  in time do :**

- $m[t] = \min(MF \times T_a [t], v[t])$  with  $T_a [t] = T[t] - T_s$
- $rfz[t] = \min(CFR \times MF \times T_n [t], vl[t])$  with  $T_n [t] = T_s - T[t]$
- $v[t+dt] = v[t] - m[t] + \text{snow}[t] + rfz[t]$

```

if  $v_l[t+dt] > CWH \times v[t+dt]$  then
     $P_{sr}^*[t] = v_l[t+dt] - CWH \times v[t+dt]$ 
     $v_l[t+dt] = CWH \times v[t+dt]$ 
else
     $P_{sr}^*[t] = 0$ 
end
end

```

---

### 3.1.2 Potential Evapotranspiration routine

An additional module allows to compute the potential evapotranspiration  $PET$  ( $\text{mm day}^{-1}$ ) based on the Oudin's formula (Oudin et al., 2005). The PET routine can be activated from the model structure area (Fig. 1 a). The PET routine affects only compartment E. The latter stands for soil and epikarst storage zone, where the water is available for actual evapotranspiration  $AET$  ( $\text{mm day}^{-1}$ ) and flows toward infiltration or surface discharge. Infiltration occurs when the water level in the compartment is greater than a given threshold  $E_{min}$ , otherwise, the compartment is considered under-saturated and does not produce infiltration. In this case, the water in compartment E is still available for evapotranspiration. KarstMod allows us to consider evapotranspiration in four separate ways (Fig. 3):

- (a) The water transfer in the soil-atmosphere continuum can be pre-processed by the user. In this case, the given precipitation time series consists of the effective precipitation  $P_{eff}$  ( $\text{mm day}^{-1}$ ), derived from precipitation  $P$  ( $\text{mm day}^{-1}$ ) and actual evapotranspiration  $AET$  ( $\text{mm day}^{-1}$ ) with Eq. 2. The evapotranspiration flux is not activated in the model structure selection panel in KarstMod (Fig. 1 a).

$P_{eff} = P - AET$	<i>Eq. 2</i>
---------------------	--------------

- (b) User-defined  $PET$  can be given as input in KarstMod for the evapotranspiration time series. Using  $E_{min}$ , the user can simulate water holding capacity and non-linear behavior of karst recharge.
- (c) User-defined  $AET$  can be given as input data in KarstMod for evapotranspiration time series instead of  $PET$ . Then, KarstMod computes an estimation of effective precipitation by limiting the evapotranspiration to water content available in compartment E. The simulated  $AET$  can then be lower than the user defined  $AET$ . Such configuration may help identifying potential inaccuracy of user defined  $AET$  for the modeling purpose but is not recommended for model set-up and parameter estimation.



154 (d) The new feature in KarstMod consists of the PET routine which estimates the PET with the Oudin's  
 155 formula (Oudin et al., 2005) (Eq. 3). It needs a  $T$  time series and two parameters to be estimated,  
 156 which can be considered in the parameter estimation procedure as well as sensitivity analysis.

$PET = \left( \frac{R_e}{\lambda \times \rho} \right) \times \left( \frac{T + K2}{K1} \right) \text{ if } T + K2 > 0 \text{ else } PET = 0$	<b>Eq. 3</b>
---	--------------

157 where  $R_e$  is the extraterrestrial radiation ( $\text{MJ m}^{-2} \text{ day}^{-1}$ ) depending only on the latitude Lat and the Julian  
 158 day,  $\lambda$  is the latent heat flux (taken equal to  $2.45 \text{ MJ kg}^{-1}$ ),  $\rho$  is the density of water (taken equal to 1000  
 159  $\text{kg m}^{-3}$ ) and  $T$  is the mean daily air temperature ( $^{\circ}\text{C}$ ).  $K1$  ( $^{\circ}\text{C}$ ) and  $K2$  ( $^{\circ}\text{C}$ ) are constants to adjust over  
 160 the catchment for rainfall-discharge model (Oudin et al., 2005). In KarstMod, both  $K1$  and  $K2$  can be  
 161 considered in the parameter estimation procedure as well as sensitivity analysis.

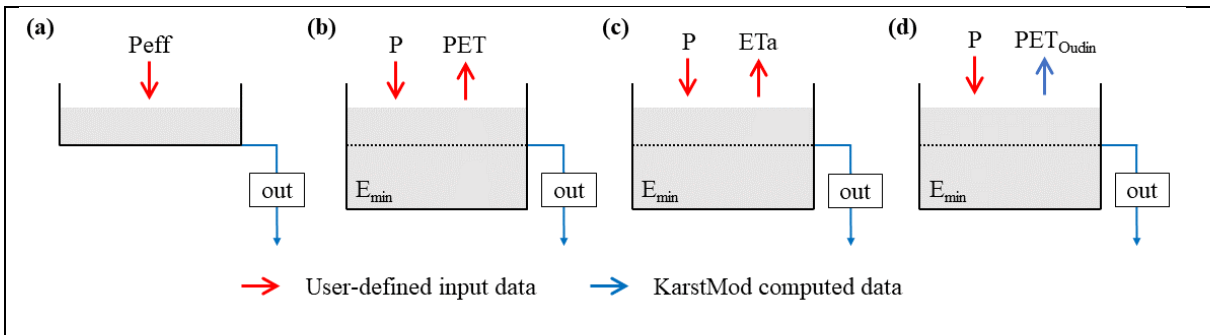


**Fig. 3** The four ways to account for evapotranspiration in KarstMod. The user can provide either (a) a self-computed effective precipitation ( $P - AET$ ) as a single input time series, (b) both  $P$  and  $PET$  time series, (c) both  $P$  and  $AET$  and (d) both  $P$  and  $T$  time series.  $P$  is precipitation,  $ET_a$  is actual evapotranspiration,  $PET$  is potential evapotranspiration and  $PET_{Oudin}$  is KarstMod's computed potential evapotranspiration with Oudin's formula.

### 162 3.2 Set-up and calibration of the model structure

163 The modular structure proposed in KarstMod is based on a widely used conceptual model which  
 164 separates karst aquifers into an infiltration zone and a saturated zone, or low and quick flows through  
 165 the unsaturated and saturated zones (Fleury et al., 2007, 2009; Guinot et al., 2015; Mazzilli et al., 2019;  
 166 Sivelles et al., 2019). Based on this conceptual representation, the platform offers four compartments  
 167 organized as a two-level structure: (i) compartment E (higher level) and (ii) compartments L, M and C  
 168 (lower level). A priori, the higher level represents the infiltration zone or the soil and epikarst. At the  
 169 lower level, compartments L, M, and C stand for the different sub-systems of the saturated zone or low  
 170 and quick flows of the whole hydro system. The various model structures and their governing equations  
 171 are presented in Mazzilli et al. (2022; 2019). Also, KarstMod allows to performance of hydrological  
 172 modeling on both daily and hourly temporal resolutions (Sivelles et al., 2019).

173 The user can activate (or deactivate) the various compartments (E, L, M, and C) within the "model  
 174 structure" panel (Fig. 1 a). The solid and faded colors represent the activated and the inactivated features,  
 175 respectively. The fluxes and their activation thresholds as well as the exponent of the discharge law  $\alpha$

176 (in case of non-linear discharge law such  $\alpha \neq 1$ ) are managed from the "model parameters" panel (Fig.  
 177 1 c). The user can account for pumping  $Q_{pump}$  (water coming out of the compartment) as well as sinking  
 178 stream  $Q_{sink}$  (water coming into the compartment). Such an option is available only if the user provides  
 179 the required time series (Fig. 1 b).

180 The user must provide warm-up, calibration, and validation periods (Fig. 1 d). The warm-up period must  
 181 be set to be independent of initial conditions to avoid bias in the parameter estimation procedure  
 182 (Mazzilli et al., 2012). Then, a calibration period (i.e. the period in which the parameters are estimated  
 183 to reduce the predictive errors) and a validation period (i.e. period separated from the calibration period)  
 184 can be defined to run the split sample test procedure (Klemeš, 1986). For calibration purpose, KarstMod  
 185 proposes several widely used performance criteria  $\phi$ : the Pearson's correlation coefficient  $R_p$   
 186 (Freedman et al., 2007), the Spearman rank correlation coefficient  $R_s$  (Freedman et al., 2007), the Nash-  
 187 Sutcliffe Efficiency NSE (Nash and Sutcliffe, 1970), the volumetric error VE (Criss and Winston, 2008),  
 188 the modified balance error BE (Perrin et al., 2001), the Kling-Gupta Efficiency KGE (Gupta et al., 2009)  
 189 and a non-parametric variant of the Kling-Gupta Efficiency KGENP (Pool et al., 2018). To compute a  
 190 multi-objective calibration procedure the user can create his objective function  $\Phi$  as a weighted sum of  
 191 several objective functions:

$\Phi = \sum_{i=1}^N \omega_i \times \phi_i(U)$	<b>Eq. 4</b>
---	--------------

192 where  $\omega_i$  is the weight affected to the objective function  $\phi_i(U)$  with  $\sum_{i=1}^N \omega_i = 1$  and  $U$  a general  
 193 notation for the observations used for parameter estimation purposes. In the KarstMod modeling  
 194 platform,  $U$  corresponds to either spring discharge  $Q_s$ , piezometric head measurements  $Z_{obs}$  (available  
 195 for compartments E, L, M, and C), or surface water discharge  $Q_{loss}$  from compartment E. Also, the  
 196 objective function  $\phi$  can be computed on transformed  $U$  to avoid high water level bias on quadratic  
 197 error. The following transformations are available in KarstMod:  $1/U$ ,  $\sqrt{U}$ ,  $1/\sqrt{U}$ . Therefore, the user  
 198 can use any combination of the objective function  $\phi$ , observations  $U$ , and variable transformations.  
 199 Depending on the modeling purpose, the user must refer to the literature to define the suitable objective  
 200 function (Bennett et al., 2013; Ferreira et al., 2020; Hauduc et al., 2015; Jackson et al., 2019).

201 The model is calibrated using a quasi-Monte-Carlo sampling procedure with a Sobol sequence sampling  
 202 of the parameter space (Sobol, 1998). The procedure involves finding an ensemble of parameter sets  
 203 providing an objective function  $\Phi$  greater than the user-defined value. The calibration procedure  
 204 stopped when either the user-defined maximum duration of the sampling procedure  $t_{max}$  is reached or  
 205 the user-defined number of parameter sets  $n_{obj}$  are collected. KarstMod offers a "run" option allowing  
 206 the model to run for a user-defined parameter set, without calibration procedure, and so allows it to  
 207 investigate "by-hand" the parameter space and the sensitivity of the model to specific parameters.



### 208 3.3 Model evaluation

209 The model performance can be evaluated for both the calibration and validation periods. It allows (i) to  
210 ensure the robustness of model predictions, even under changing conditions (which is a key point for  
211 the assessment of climate change impact) and (ii) to avoid model over-fitting within a specific range of  
212 hydro-climatic conditions observed during the calibration period. KarstMod allows the computation of  
213 the above-mentioned performance criteria for both calibration and validation periods. Even though the  
214 notation "validation" is disputable such a procedure is required to evaluate both explanatory and  
215 predictive dimensions of the model structure (Andréassian, 2023). Then, KarstMod offers an ensemble  
216 of numerical tools devoted to (i) checking the model consistency, i.e. explanatory dimension of the  
217 model (Beven, 2001; Shmueli, 2010), (ii) evaluating the model performance, i.e. predictive dimension  
218 of the model structure.

219 To check the model consistency, the simulation based on the parameter set that provides the highest  
220 objective function value can be analyzed through an ensemble of graphs such as (i) internal and external  
221 fluxes as a function of time, (ii) cumulative volumes for both observed and simulated time series for  
222 spring discharge  $Q_s$  and surface water discharge  $Q_{loss}$ , (iii) simulated mass-balance as a function of  
223 time, (iv) comparison of observations and simulations for either  $Q_s$  or  $Q_{loss}$  with probability function  
224 plots, auto-correlogram of the spring discharge time series, cross-correlogram of precipitation-discharge  
225 time series.

226 To evaluate the model performance, KarstMod offers a "Model evaluation" panel available from the  
227 graphs panel (Fig. 1 g) that includes several sub-panels, from the left to the right:

- 228 • The diagnostic efficiency DE (Schwemmler et al., 2021) which consists of a diagnostic polar plot  
229 that facilitates the model evaluation process as well as the comparison of multiple simulations. The  
230 DE accounts for constant, dynamics, and timing errors, and their relative contribution to the model  
231 errors. Also, the decomposition of the errors between the periods of high flows and low flows allows  
232 us to better investigate the model bias, as well as to provide critical evaluation for impact studies,  
233 particularly for the assessment of climate change impacts. Indeed, the accurate evaluation of low  
234 flow periods (in terms of frequency, intensity, and duration) becomes increasingly crucial for  
235 groundwater resource variability assessment.
- 236 • The available objective functions  $\Phi$  are presented as a radar chart which consists of a polygon where  
237 the position of each point from the center gives the value of the performance criteria. The closer the  
238 point is to the outside of the radar chart, the better the model performs. The radar chart is made for  
239 both calibration and validation periods and each of the calibration variables considered in the  
240 modeling ( $Q_s$ ,  $Z_{obsA}$  with A for either E, M, C or L compartments and  $Q_{loss}$ ).
- 241 • The KGE (Gupta et al., 2009) consists of a diagonal decomposition of the NSE (Nash and Sutcliffe,  
242 1970) to separate Pearson's correlation coefficient  $R_p$ , representation of bias  $\beta_{KGE}$ , and variability

243  $\alpha_{KGE}$ . Thus, the  $KGE$  is comparable to multi-objective criteria for calibration purposes  
244 (Pechlivanidis et al., 2013). The sub-panel offers (i) a bi-plot of the three  $KGE$ 's components and  
245 (ii) a radar plot visualization of the  $KGE$ 's components, allowing the identify potential  
246 counterbalancing errors according to these different components (Cinkus et al., 2023b). The two  
247 above-mentioned plots also include the decomposition of the  $KGENP$  (Pool et al., 2018) in terms of  
248 Spearman's rank correlation coefficient  $R_s$ , representation of bias  $\beta_{KGENP}$  and non-parametric  
249 variability  $\alpha_{KGENP}$ .

### 250 **3.4 Dealing with uncertainties**

251 Moges et al. (2021) summarize the various sources of uncertainties in hydrological models including  
252 structural and parametric uncertainties as well as uncertainties related to input data and observations.  
253 The latter concerns both the input (i.e., precipitation and evapotranspiration) and the output (i.e.,  
254 discharge) of the modeled systems. Many references are devoted to the uncertainties related to input  
255 data and observations. As an example, Westerberg et al. (2020) include information about the discharge  
256 uncertainty distribution in the objective function and perform better discharge simulation. Also, the  
257 precipitation error can be dependent on the data time step (McMillan et al., 2011) and could impact the  
258 hydrological model performance (Ficchi et al., 2016). Lumped parameter hydrological models consider  
259 meteorological time series representative of a whole catchment, which may require some pre-processing,  
260 particularly for snow processes since it can have a strong influence on flow dynamics. Thus, KarstMod  
261 includes variables related to both the snow routine (i.e., the redistributed precipitation time series  $P_{sr}$ )  
262 and the PET routine (i.e., estimated potential evapotranspiration  $PET$ ) in the parameter estimation  
263 procedure. This allows us to investigate the sensitivity of the flow simulation to these input data when  
264 using snow and PET routines. Nonetheless, KarstMod does not include features to investigate the impact  
265 of observation uncertainties on parameter estimation.

266 As with many environmental problems, parameter estimation in rainfall-discharge modeling consists  
267 generally of ill-posed problems, i.e. the modeling encounters issues about the unicity, identifiability, and  
268 stability of the problem solution (Ebel and Loague, 2006). As a consequence, several representations of  
269 the modeled catchment may be considered equally acceptable (Beven, 2006). Knoblen et al. (2020)  
270 evaluate the performance of 36 daily lumped parameter models over 559 catchments and show that  
271 between 1 and up to 28 models can show performance close to the model structure with the highest  
272 performance criteria. Such results are widely covered in catchment hydrology (Dakhlaoui and Djebbi,  
273 2021; Darbandsari and Coulibaly, 2020; Gupta and Govindaraju, 2019; Pandi et al., 2021; Zhou et al.,  
274 2021) but still poorly investigated in karst hydrology. Indeed, the structural uncertainty impacts on  
275 rainfall-discharge modeling in karst hydrology is not properly evaluated whereas many studies consider  
276 several hydrological model structures to include structural uncertainty in flow simulation (Hartmann et  
277 al., 2012; Jiang et al., 2007; Jones et al., 2006; Sivelse et al., 2021). KarstMod includes more than fifty  
278 combinations of the various compartments as well as various compartments model (i.e., compartment

279 with linear or non-linear discharge law and compartment with infinite characteristic time) and allows a  
280 quick implementation of the various model structures. The user can easily manage to start the modeling  
281 with one single compartment and gradually move to a more complex model structure with up to four  
282 compartments, five fluxes connected to the spring, four internal fluxes, and 1 flux running out of the  
283 system.

284 Considering each model structure, parametric equifinality can be investigated using (i) dot plots of the  
285 values of the objective function against the parameter values, (ii) dot plots of the values of the  
286 performance criteria used to define the aggregated objective function, and (iii) the variance-based, first-  
287 order  $S_i$  and total  $ST_i$  sensitivity indexes for the model parameters. Details concerning the computation  
288 of sensitivity indexes within KarstMod are given in Mazzilli et al. (2022; 2019).

## 289 **4 Examples of application**

290 To illustrate the KarstMod application and the use of the above-presented functionalities for the  
291 assessment of karst groundwater resources, we propose two case studies: (i) the Touvre karst system  
292 and (ii) the Lez karst system. Both karst systems consist of strategic freshwater resources for drinking  
293 water supply (DWS), for the city of Angoulême (western France) and Montpellier (southern France)  
294 respectively.

### 295 **4.1 The Touvre karst system (La Rochefoucauld)**

296 The Touvre is a karst system where the infiltration consists of (i) a delayed infiltration of effective  
297 precipitation on the karstic recharge area and (ii) a direct infiltration of surface water from the Tardoire,  
298 Bandiat, and Bonnieure rivers. The latter are surface streams flowing on metamorphic rocks that partly  
299 infiltrate to subterranean at the contact with carbonate formations, mainly composed of Middle to Upper  
300 Jurassic limestones. The springs of the Touvre, located 7 km east of Angoulême (western France), counts  
301 four outlets, namely the Bouillant, the Dormant, the Font de Lussac, and the Lèche (Labat et al., 2022).  
302 In the following, the Touvre Spring discharge designates the accumulated discharge of the four  
303 mentioned outlets.

304 The Touvre karst system constitutes a strategic freshwater resource for the DWS of Angoulême, with  
305 around 110,000 inhabitants, but also contributes to the water supply for industry and agriculture. In  
306 2015, there were eighty-four pumping wells over the karstic impluvium of the Touvre karst system, and  
307 around one hundred more in the Tardoire, Bandiat, and Bonnieure rivers catchment. Based on the data  
308 provided by the Adour-Garonne Water Agency, the annual groundwater abstraction for agriculture  
309 represents 4.6 Mm<sup>3</sup> whereas annual groundwater abstraction for DWS represents 1.1 Mm<sup>3</sup> over the  
310 karstic impluvium of the Touvre karst system. On the three rivers catchment (out of the karstic  
311 impluvium), the annual groundwater abstraction represents 2.5 Mm<sup>3</sup> for agriculture and 3.3 Mm<sup>3</sup> for  
312 DWS, through river intakes or alluvial groundwater abstraction. The total annual volume of abstracted  
313 groundwater in the area represents around 5 % of the annual volume of transit at the Touvre Spring.

314 This is quite low compared with karst aquifers in France exploited for their groundwater resources, such  
315 as the Lez spring (Jourde et al., 2014) and the Oeillal's spring karst catchment (Sivelle et al., 2021),  
316 where the annual groundwater abstraction volume represents respectively 50 % and 15 % of the annual  
317 volume of transit at the spring. Therefore, the Touvre karst system seems not to be over-exploited at the  
318 moment, but the impact of groundwater abstraction should be addressed in the context of global change  
319 to ensure sustainable management of this strategic freshwater resource.

320 The area is characterized by an ocean-influenced climate with a mean annual precipitation of around  
321 800 mm year<sup>-1</sup> distributed over an average of 255 rainy days. The estimation is performed with Thiessen  
322 polygon methods based on eleven meteorological stations over the area (Labat et al., 2022). The mean  
323 annual potential evapotranspiration is around 770 mm year<sup>-1</sup> according to the Penman-Monteith  
324 estimation provided by the French meteorological survey (Météo-France). The Touvre daily spring  
325 discharge shows a significant variability ranging from 3 m<sup>3</sup> s<sup>-1</sup> to 49 m<sup>3</sup> s<sup>-1</sup> with a coefficient of variation  
326 around 0.46 (Fig. 5 b).

327 The surface stream flow rates for the Bonnieure, Bandiat, and Tardoire rivers are concentrated within  
328 the autumn and winter periods. During the summer period, the discharge in the three rivers is very low  
329 (Fig. 5 c). The more significant groundwater abstraction is performed during the summer period, while  
330 the Touvre spring discharge reaches its lowest values within the late summer and early autumn periods  
331 (Fig. 5, c and d).

332 Fig. 4 shows the model structure for the Touvre karst system that consists of three compartments  
333 organized in two levels (Labat et al., 2022). The upper level corresponds to reservoir E and represents  
334 both the unsaturated part of the system and a temporary aquifer. This reservoir relates to the two  
335 reservoirs of the lower level: C (Conduit) and M (Matrix) representative of quick and slow flow  
336 dynamics, respectively. The upper level of the model structure is affected by *P* and *ET* while the lower  
337 level of the model structure is affected by (i) groundwater abstraction and (ii) sinking river streamflow  
338 from the surface to underground. Fig. 4 shows the various time series required for the hydrological  
339 modeling of the Touvre karst system. The methodology for daily time series preparation given in Labat  
340 et al. (2022) allows us to account for the influence of groundwater abstraction on the transmissive or  
341 capacitive part of the karst aquifer as well as the influence of concentrated and diffuse infiltration of the  
342 surface river streamflow.

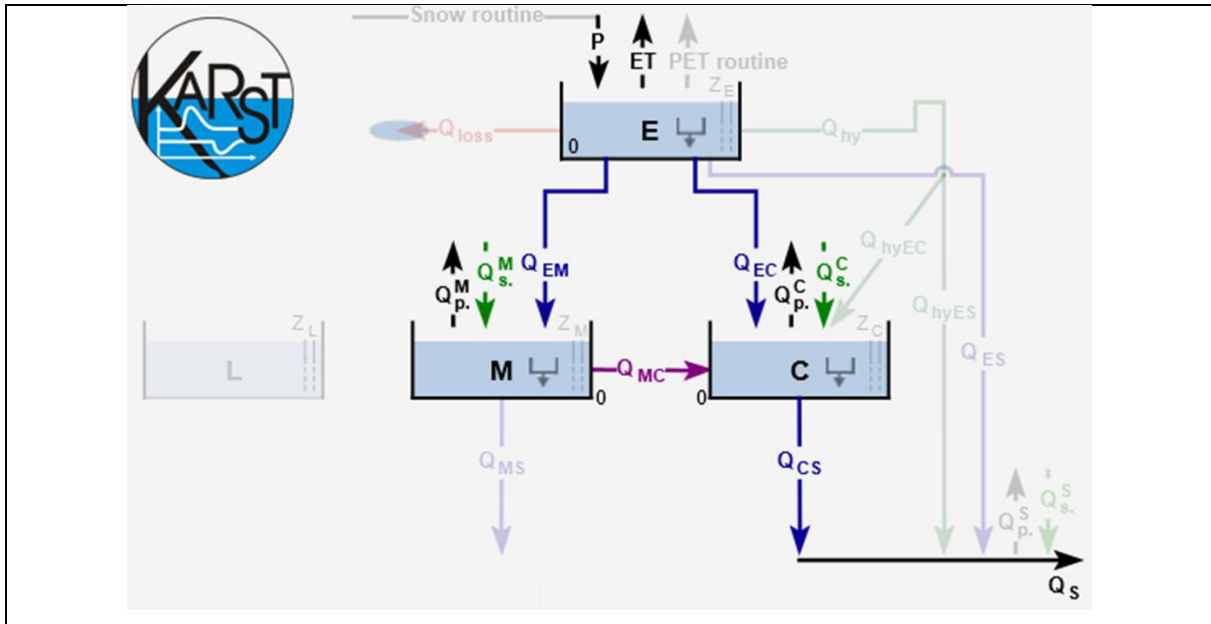


**Fig. 4 Screenshot of KarstMod with a focus on the panel "Model structure" for the Touvre karst system. The solid lines correspond to the activated fluxes whereas the faded color lines are not activated.  $Q_p^M$  and  $Q_p^C$  stand for groundwater abstraction that affects compartments M and C respectively while  $Q_s^M$  and  $Q_s^C$  stand for sinking flow that affects compartments M and C respectively.**

343

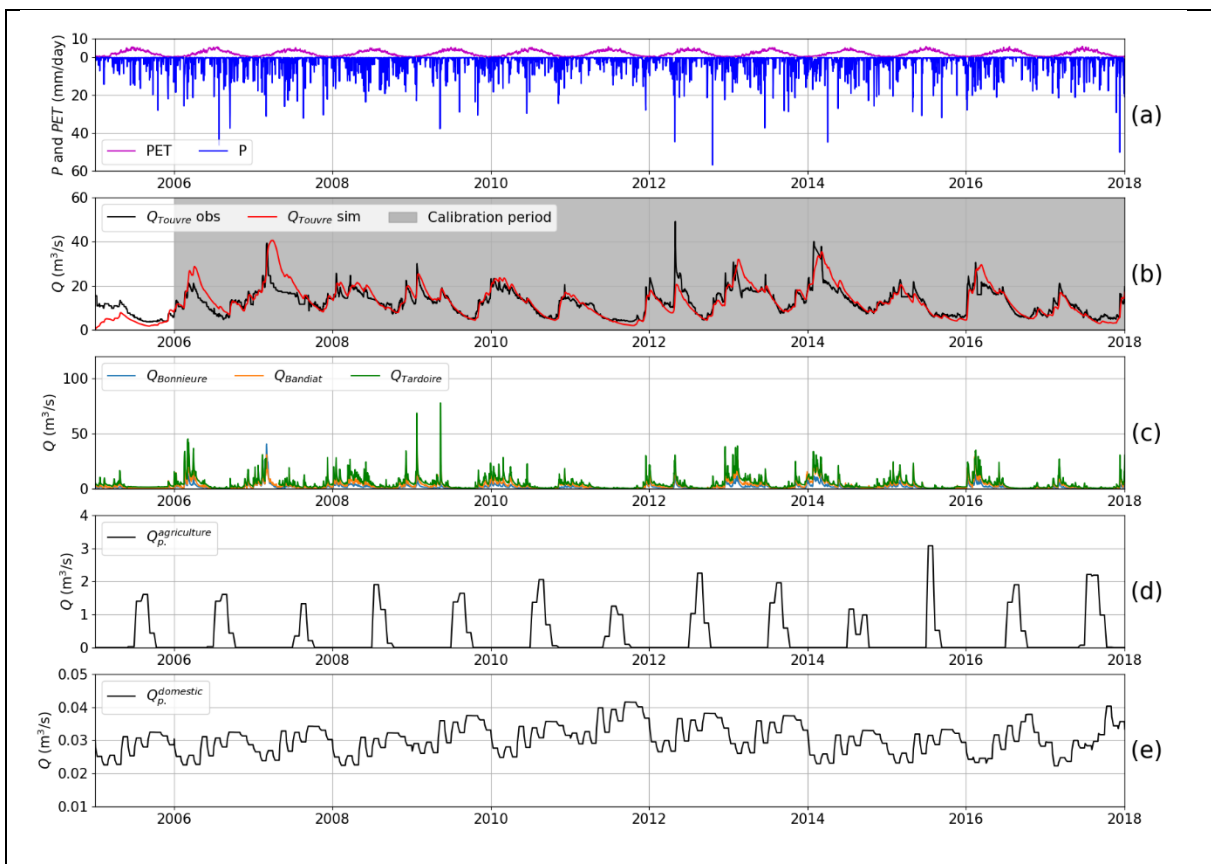


**Fig. 5 Daily time series for the Touvre system: a) precipitation (P) and potential evapotranspiration (PET), b) observed and simulated karst spring discharge ( $Q_{Touvre\ obs}$  and  $Q_{Touvre\ sim}$ ), c)**

*observed river streamflow discharge ( $Q_{Bonnieur}$ ,  $Q_{Bandiat}$ ,  $Q_{Tardoire}$ ),  $d$ ) and  $e$ ) groundwater abstraction discharge ( $Q_p^{agriculture}$ ,  $Q_p^{domestic}$ ).*

344 The objective of the hydrological modeling is to assess the impact of groundwater abstraction on spring  
 345 discharge, more particularly during low flow periods (Labat et al., 2022). So, the calibration is performed  
 346 according to the *KGENP* that improves the simulations during mean and low-flow conditions using the  
 347 Spearman rank correlation due to its insensitivity to extreme values (Pool et al., 2018). The sampling  
 348 procedure is set up to find  $n_{obj} = 5000$  simulations with *KGENP* greater than 0.9. Afterwards, the model  
 349 is evaluated using the various features proposed in KarstMod (Fig. 6). The diagnostic efficiency plot  
 350 (Fig. 6 a) testifies of several elements: (i) the model seems to slightly overestimate high flow and  
 351 underestimate low flow, (ii) the timing error is about 0.9, testifying of suitable flow dynamics in the  
 352 model, (iii) low flow periods contribute more to the model errors, and (iv) there is no offset in the  
 353 simulated spring hydrograph. The radar chart (Fig. 6 b) shows a good equilibrium between the various  
 354 objective functions whose values are greater than 0.8, except for the NSE criteria (NSE = 0.75). It is the  
 355 consequence of the design of these criteria that tends to outweigh the errors during floods. Here the NSE  
 356 value is still greater than 0.7 and testifies to a "very good" fit according to Moriasi et al. (2007). Finally,  
 357 the decomposition of the KGE (Fig. 6 c and d) shows  $R_p = 0.91$ ,  $\alpha = 1.15$  and  $\beta = 1.02$  testifying of  
 358 accurate dynamics and low bias, but slightly too high variability.

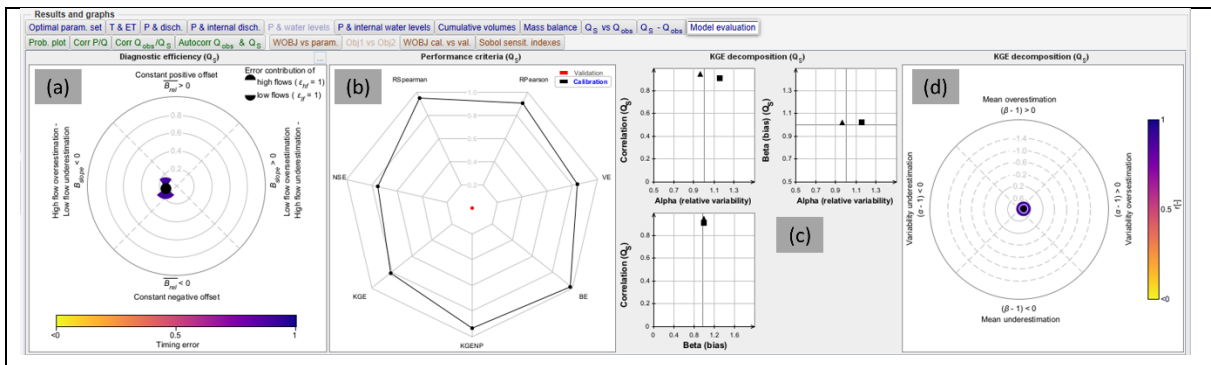


**Fig. 6 Screenshot of KarstMod with a focus on the sub-panel "Model evaluation". Application for the model evaluation on the Touvre system: (a) diagnostic efficiency plot (Schwemmler et al., 2021), (b) radar chart of the objective functions, (c) bi-plot of the KGE's (square) and KGENP's (triangle) components, and (d) radar chart of the KGE's components.**

## 359 4.2 The Lez Spring

360 The Lez Spring (southern France) consists of the main outlet of a karst system encompassed in the North  
 361 Montpellieran Garrigue hydrogeological unit delimited to the west by the Herault River, and to the north  
 362 and east by the Vidourle River. The geology in the area corresponds to the Upper Jurassic layers  
 363 separated by the Corconne-Matelle fault (oriented N30°), leading to two main compartments in the  
 364 aquifer (Bérard, 1983; Clauzon et al., 2020). The karst aquifer is unconfined in the western compartment  
 365 and is locally confined in the eastern compartment. The Lez Spring is located about 15 km north of  
 366 Montpellier. It is of Vauclusian-type with an overflow level at 65 m a.s.l and a maximum daily discharge



367 of approximately  $15 \text{ m}^3 \text{ s}^{-1}$ . The area is characterized by a typical Mediterranean climate with dry  
368 summers and rainy autumns. Over the 2009-2019 period, the mean annual precipitation is around 900  
369  $\text{mm year}^{-1}$  distributed over an average of 133 rainy days (estimation with Thiessen polygon methods  
370 based on four meteorological stations over the area: Prades-le-Lez, Saint-Martin-de-Londres,  
371 Sauteyrargues, and Valflaunès), a mean annual potential evapotranspiration is around 900  $\text{mm year}^{-1}$   
372 according to the estimation based on Oudin's formula with the temperature measured at Prades le Lez  
373 station while the real annual evapotranspiration is around 450  $\text{mm year}^{-1}$  (eddy covariance flux-station  
374 of Puéchabon).

375 Since 1854, the Lez Spring supplies the drinking water to Montpellier city and the surroundings. It  
376 currently constitutes the main freshwater resource for around 350,000 people in the area. The present  
377 water management scheme allows pumping at higher rates than the natural spring discharge during low  
378 flow periods, while supplying a minimum discharge rate (around  $0.23 \text{ m}^3 \text{ s}^{-1}$ ) into the Lez River to ensure  
379 ecological flow downstream, and reducing flood hazards via rainfall storage in autumn (Avias, 1995;  
380 Jourde et al., 2014). The pumping plant was built in 1982 with four deep wells drilled to intercept the  
381 karst conduit feeding the spring, 48 m below the overflow level of the spring. Pumping in these wells  
382 allows up to  $0.18 \text{ m}^3 \text{ s}^{-1}$  to be withdrawn under low flow periods (with an authorized maximum  
383 drawdown of 30 m), while the average annual pumping flow rate is about  $0.10 \text{ m}^3 \text{ s}^{-1}$  (over the 2008-  
384 2019 period). Due to the pumping management of the aquifer, which supplies about 30 to 35  $\text{Mm}^3$  of  
385 water per year to the metropolitan area of Montpellier, the discharge at the Lez Spring is often low or  
386 nil. Discharge is also measured downstream (Lavalette gauging station) where the measured discharge  
387 corresponds to the Lez Spring discharge and the main tributaries (Lirou and Terrieu streams) which flow  
388 essentially after intense Mediterranean rainfall events. As suggested in Cousquer and Jourde (2022), the  
389 surface water discharge, denoted  $Q_{loss}$ , can be estimated as the difference between the total discharge  
390 in Lavalette and the Lez spring discharge.

391 In the present context of global change, Mediterranean karst systems already show significant decrease  
392 in spring discharge (Doummar et al., 2018; Dubois et al., 2020; Fiorillo et al., 2021; Hartmann et al.,  
393 2012; Nerantzaki and Nikolaidis, 2020; Smiatek et al., 2013) which could be aggravated with  
394 groundwater abstraction (Sivelle et al., 2021). The Lez spring is strongly exposed to global change  
395 impact: (i) the Mediterranean area is identified as a climate change hot-spot (Diffenbaugh and Giorgi,  
396 2012) where the projected warming spans 1.8–8.4°C according to CMIP6 and 1.2–6.6°C according to  
397 CMIP5 during the summer period (Cos et al., 2022), and (ii) the water management scheme will have  
398 to adapt to the future need in drinking water for the growing population in the area as well as changes  
399 in the freshwater consumption practice (e.g. water use restriction order). Therefore, a sustainable water  
400 management plan for the Lez Spring requires a good appreciation of the hydrological functioning as  
401 well as the operational hydrological model to properly address impact studies. In this framework,  
402 KarstMod allows for choosing and calibrating a suitable model structure. This constitutes the first step

403 for a global change impact study that requires prediction tools to simulate the aquifer response to various  
 404 external forces.

405 Fig. 7 shows the model structure for the Lez karst catchment (Mazzilli et al., 2011) that consists of three  
 406 compartments organized in two levels. The upper level corresponds to compartment E and represents  
 407 the unsaturated part of the system, including a soil water holding capacity  $E_{min}$  and a discharge lost  
 408 from the compartment  $Q_{loss}$ . **Compartment E** is exposed to  $P$  and  $ET$  and discharge towards the lower  
 409 level of the model structure starts when the water level exceeds  $E_{min}$ . The lower level consists of two  
 410 inter-connected compartments M and C allowing to reproduction of the lateral exchanges, denoted  $Q_{MC}$ ,  
 411 between the transmissive function (compartment C) and the capacitive function (compartment M) of the  
 412 karst aquifer. Both M and C compartments are considered bottomless, allowing to reproduce periods of  
 413 non-overflow at the **Lez Spring** when the mean water level in the aquifer stands below 65 m a.s.l., mainly  
 414 during summer periods due to pumping in the karst conduit. Fig. 8 a and b show the various daily time  
 415 series required for the hydrological modeling of the Lez karst system (*i.e.*,  $P$ ,  $ET$  and  $Q_{pump}$ ).

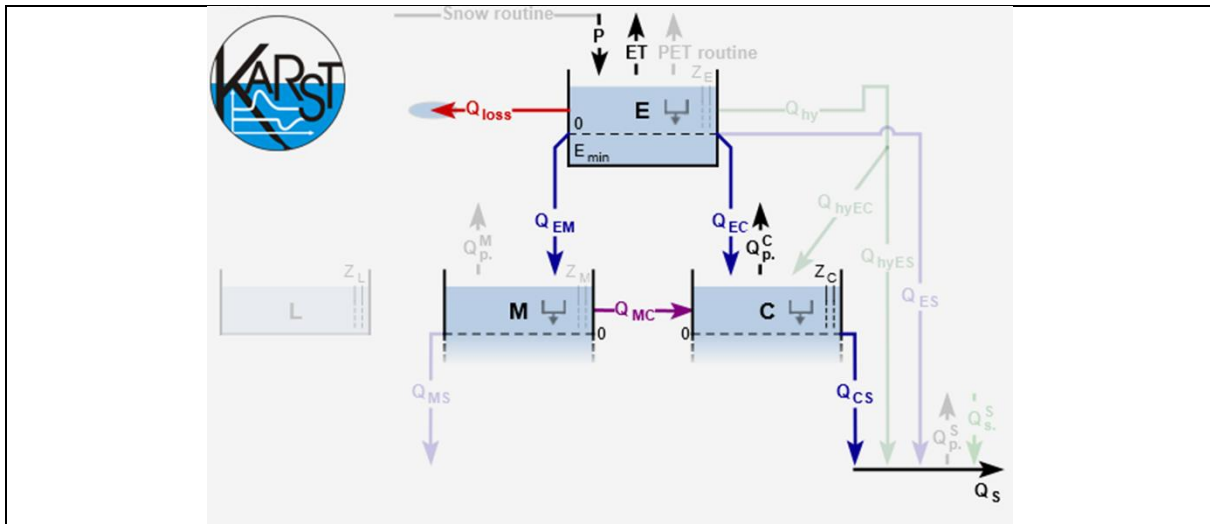


**Fig. 7 Screenshot of KarstMod with a focus on the panel "Model structure" for the Lez karst system. The solid lines correspond to the activated fluxes whereas the faded color lines are not activated.  $Q_{loss}$  stands for the surface water discharge from the epikarst compartment,  $Q_p^C$  stands for groundwater abstraction that affects compartments C while  $Z_C$  stands for piezometric head measurements considered as representative of **compartment C**.**

416

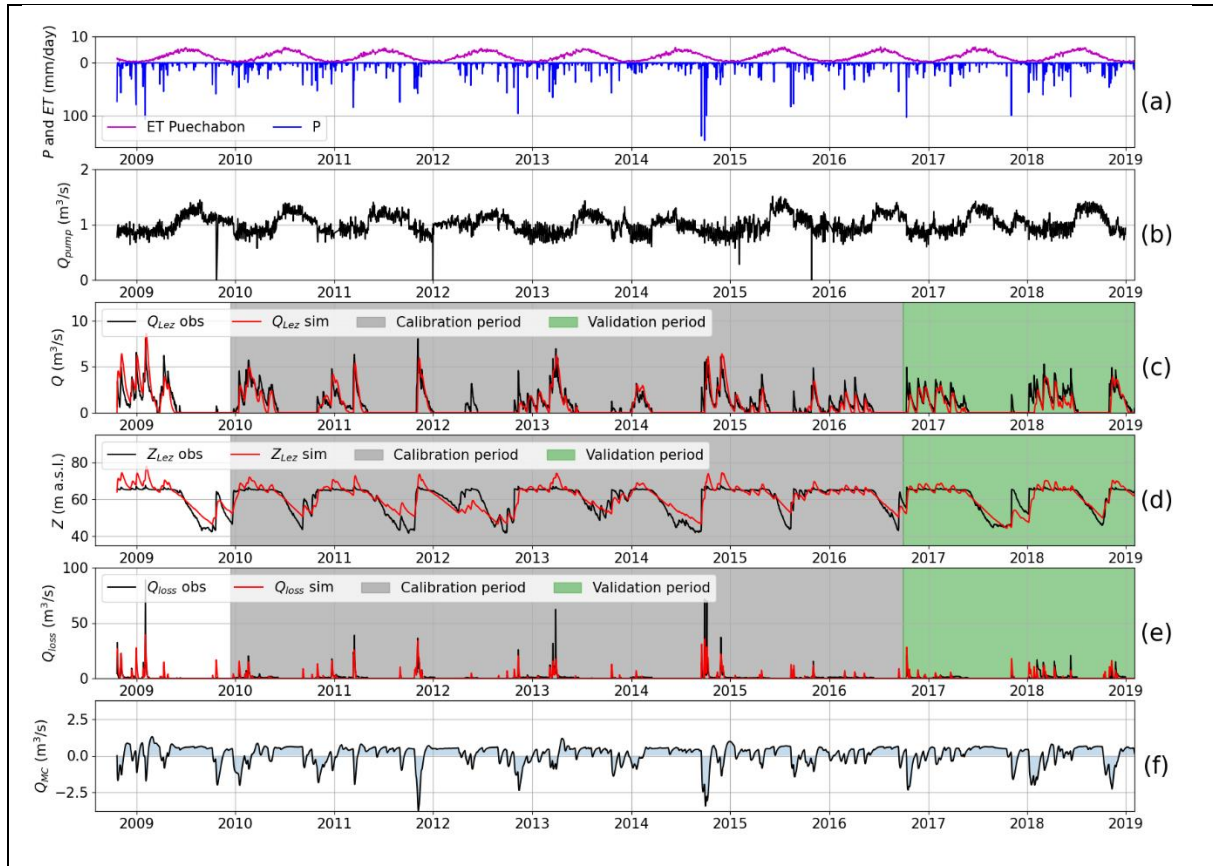


**Fig. 8 Daily time series for the Lez system: a) precipitations ( $P$ ) and evapotranspiration ( $ET$ ), b) groundwater abstraction,  $Q_{pump}$ , c) observed and simulated karst spring discharge ( $Q_{Lez\ obs}$  and  $Q_{Lez\ sim}$ ), d) observed and simulated piezometric head ( $Z_{Lez\ obs}$  and  $Z_{Lez\ sim}$ ), e) surface water discharge ( $Q_{loss}$ ) and f) simulated exchanges fluxes between compartment M and C,  $Q_{MC}$ .**

417 The available hydrological observations for model calibration consist of spring discharge  $Q_S$ ,  
 418 piezometric head measurement  $Z_C$  at the Lez spring, and surface water discharge from secondary outlets  
 419 and intermittent springs  $Q_{loss}$  (Fig. 8 c, d, and e).

420 The surface water discharge is estimated as the difference in discharge measured at the Lavalette station  
 421 (15 km downstream of the Lez spring) and the discharge measured at the Lez spring, as proposed by  
 422 Cousquer and Jourde (2022). Therefore,  $Q_{loss}$  includes all the water loss from the epikarst within several  
 423 seasonal overflowing springs (i.e., Lirou spring, Restinclière spring, and Fleurette spring). KarstMod  
 424 allows for easy handling of the various parameter estimations depending on the considered hydrological  
 425 observations (i.e., spring discharge, piezometric head measurement, and surface discharge from the  
 426 epikarst). The sampling procedure is set up to find  $n_{obj} = 5000$  simulations with an aggregated objective  
 427 function  $\Phi$  greater than 0.6. As suggested by Cousquer and Jourde (2022), using complementary  
 428 hydrological observations in addition to the spring discharge allows for to reduce the parametric  
 429 uncertainties in the modeling of the Lez spring discharge. Therefore, using a multi-objective calibration  
 430 procedure implemented in KarstMod, the objective function is built such as:

$$\Phi = \frac{1}{3} \times NSE(Q_s) + \frac{1}{3} \times NSE(Z_c) + \frac{1}{3} \times NSE(Q_{loss})$$

**Eq. 5**

431 The calibration procedure leads to an optimal  $\Phi = 0.65$  decomposed such as  $\phi Q_s = 0.70$ ,  $\phi Z_c = 0.57$   
 432 and  $\phi Q_{loss} = 0.70$  within the calibration period. Model performance evaluation on the validation period  
 433 shows suitable model performance for both spring discharge and piezometric with  $\phi Q_s = 0.54$  and  $\phi Z_c$   
 434  $= 0.79$ , but poor model performance according to the surface water discharge with  $\phi Q_{loss} = 0.36$ .  
 435 Afterwards, the results can be evaluated using the various features proposed in KarstMod (Fig. 9). The  
 436 results show higher model performances for  $Q_s$  and  $Z_c$  than for  $Q_{loss}$ . The model performance appears  
 437 quite satisfactory concerning the variable of interest to assess the impact of the water management  
 438 scheme on the groundwater resources within the Lez aquifer.

439 The simulated exchange fluxes between compartments M and C (Fig. 8 f) show consistent dynamics  
 440 with the observations. Indeed, during periods of high flow, the exchange fluxes are oriented from  
 441 compartment C to compartment M (i.e.,  $Q_{MC} < 0$ ). Significant precipitation events lead to rapid rises in  
 442 the piezometric head, saturation of the transmissive part of the aquifer, and finally the establishment of  
 443 overflow at the Lez spring (i.e.  $Q_s > 0$ ) as well as the overflowing springs (i.e.  $Q_{loss} > 0$ ). Conversely,  
 444 during the periods of low piezometric head (i.e., both  $Q_s$  and  $Q_{loss}$  are nil), the simulated exchange  
 445 fluxes are oriented from compartment M to compartment C (i.e.  $Q_{MC} > 0$ ). Such flow exchanges between  
 446 capacitive and transmissive parts of karst aquifers have been evidenced using KarstMod on other karst  
 447 environment (Duran et al., 2020; Frank et al., 2021; Labat et al., 2022; Sivelles et al., 2019).

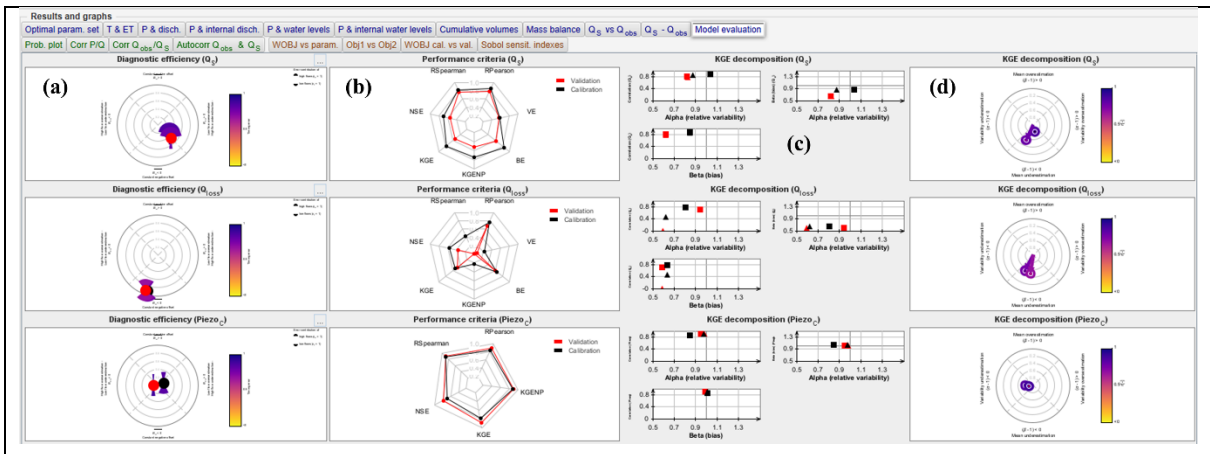


**Fig. 9 Screenshot of KarstMod with a focus on the sub-panel "Model evaluation". Application for the model evaluation on the Lez system. The panel is composed such as (i) each row corresponds to the variable for calibration ( $Q_s$ ,  $Q_{loss}$  and  $PiezoC$ ) and (ii) each column corresponds to (a) diagnostic efficiency plot, (b) radar plots, one should note that VE and BE are not computed according to the piezometric time series, (c) decomposition of KGE (square) and KGENP (triangle) and (d) radar plot of the KGE decomposition.**

## 448 5 Conclusion

449 KarstMod consists of a useful tool for the assessment of karst groundwater variability and sensitivity to  
450 anthropogenic pressures (e.g., groundwater abstraction). This tool is devoted to promoting good  
451 practices in hydrological modeling for learning and occasional users. KarstMod requires no  
452 programming skills and offers a user-friendly interface allowing any user to easily manage hydrological  
453 modeling. As a first step, KarstMod can be used to explore the ability of conceptual representations to  
454 explain observations such as discharge or piezometric heads in karst systems. More advanced use of  
455 KarstMod is also possible as it provides a complete framework for (i) primary analysis of the data, (ii)  
456 comparison of various model structures, (iii) evaluation of the hydrological model performance as well  
457 as (iv) first assessment of parametric uncertainties. The research community increasingly uses KarstMod  
458 to address various challenges in karst hydrology, from understanding hydrological processes to practical  
459 applications such as evaluation of groundwater management plans, or even assessment of the impact of  
460 groundwater abstraction and climate changes on karst groundwater resources.

461 Future developments of KarstMod might include (i) the consideration of the spatial heterogeneity in  
462 recharge processes which is essential when considering snowmelt as well as land cover (Sivelle et al.,  
463 2022a), (ii) the simulation of electrical conductivity (Chang et al., 2021), major ions concentration  
464 (Hartmann et al., 2013) or natural tracer such as air excess (Sivelle et al., 2022a), and (iii) the assessment  
465 of structural uncertainty (Cousquer et al., 2022). KarstMod should tend toward an open source research  
466 software to avoid duplication of efforts in karst hydrological modeling. Also, a Python version is  
467 required for a better connection with an additional framework for sensitivity analysis such as SAFE  
468 toolbox (Pianosi et al., 2015) and for model calibration procedures such as particle swarm optimization  
469 (Eberhart and Kennedy, 1995; Lee, 2014). Finally, the development of the KarstMod modeling platform  
470 will benefit better transparency and repeatability with an open-source approach, as observed on other  
471 numerical tools (Pianosi et al., 2020).

### 472 Nomenclature.

<i>AET</i>	<u>actual evapotranspiration (mm day<sup>-1</sup>)</u>
<i>CFR</i>	<u>refreezing coefficient (-)</u>
<i>CWH</i>	<u>liquid water holding capacity of snow (-)</u>
<i>DE</i>	<u>diagnostic efficiency DE (Schwemmler et al., 2021)</u>
<i>ET</i>	<u>evapotranspiration (mm day<sup>-1</sup>)</u>
<i>KGE</i>	<u>Kling-Gupta Efficiency (Gupta et al., 2009)</u>
<i>KGEP</i>	<u>non-parametric Kling-Gupta Efficiency (Pool et al., 2018)</u>
<i>MF</i>	<u>melt coefficient (mm °C<sup>-1</sup> day<sup>-1</sup>)</u>
<i>P</i>	<u>precipitation (mm day<sup>-1</sup>)</u>
<i>P<sub>eff</sub></i>	<u>effective precipitation (mm day<sup>-1</sup>)</u>

$P_{SR}$	<u>precipitation computed with the Snow Routine (mm day<sup>-1</sup>)</u>
$P_{SR}^*$	<u>precipitation for a single sub-catchment computed with the Snow Routine (mm day<sup>-1</sup>)</u>
$PET$	<u>potential evapotranspiration (mm day<sup>-1</sup>)</u>
$R_p$	<u>Pearson's correlation coefficient</u>
$R_s$	<u>Spearman rank correlation coefficient</u>
$NSE$	<u>Nash-Sutcliffe Efficiency (Nash and Sutcliffe, 1970)</u>
$n_{obj}$	<u>targeted number of parameter sets</u>
$Q_A$	<u>water discharge considered for the flow component A (m<sup>3</sup> s<sup>-1</sup>)</u>
$T$	<u>air temperature (°C)</u>
$T_a$	<u>active temperature for snowmelt (°C)</u>
$T_n$	<u>active temperature for refreezing (°C)</u>
$t_{max}$	<u>maximum duration for sampling the parameter space (seconds)</u>
$T_s$	<u>temperature threshold (°C)</u>
$U$	<u>observations considered for parameter estimation</u>
$VE$	<u>volumetric error (Criss and Winston, 2008)</u>
$Z_A$	<u>water level considered for element A (m a.sl.)</u>
$\phi$	<u>performance criteria</u>
$\Phi$	<u>objective function</u>

473 Code availability. The KarstMod modeling platform is developed and made freely accessible within the  
474 framework of the KARST observatory network (SNO KARST) initiative from the INSU/CNRS. The  
475 platform can be downloaded here: <https://sokarst.org/en/software-en/karstmod-en/>

476 Author contributions. V. Sivelles: methodology, software, writing—original draft. G. Cinkus:  
477 methodology, software, writing—review, and editing. N. Mazzilli: methodology, software, project  
478 administration, writing—review and editing. H. Jourde: methodology, software, project administration,  
479 funding acquisition, writing—review and editing. D. Labat: methodology, software, writing—review,  
480 and editing. B. Arfib: methodology, software, writing—review and editing. N. Massei: methodology,  
481 software, writing—review and editing. Y. Cousquer: writing—review and editing. D. Bertin:  
482 methodology, software, writing—review, and editing.

483 Competing interests. The authors declare no competing interest.

484 Acknowledgements. This platform is developed within the framework of the KARST observatory  
485 network (SNO KARST) initiative from the INSU/CNRS (France), which aims to strengthen knowledge-  
486 sharing and promote crossdisciplinarity in research on karst systems at the national scale. This work, as  
487 well as V. Sivelles's post-doctoral position, was supported by the European Commission through the



488 Partnership for Research and Innovation in the Mediterranean Area (PRIMA) program under Horizon  
489 2020 (KARMA project, grant agreement number 01DH19022A).

490 **References**

- 491 Andréassian, V.: On the (im)possible validation of hydrogeological models, *Comptes Rendus.*  
492 *Géoscience*, 355, 1–9, <https://doi.org/10.5802/crgeos.142>, 2023.
- 493 Avias, J. V.: Gestion active de l'exurgence karstique de la Source du Lez (Hérault, France) 1957-1994,  
494 *Hydrogéologie (Orléans)*, 113–127, 1995.
- 495 Bailly-Comte, V., Martin, J. B., Jourde, H., Sreaton, E. J., Pistre, S., and Langston, A.: Water exchange  
496 and pressure transfer between conduits and matrix and their influence on hydrodynamics of two karst  
497 aquifers with sinking streams, *Journal of Hydrology*, 12, 2010.
- 498 Bennett, N. D., Croke, B. F. W., Guariso, G., Guillaume, J. H. A., Hamilton, S. H., Jakeman, A. J.,  
499 Marsili-Libelli, S., Newham, L. T. H., Norton, J. P., Perrin, C., Pierce, S. A., Robson, B., Seppelt, R.,  
500 Voinov, A. A., Fath, B. D., and Andreassian, V.: Characterising performance of environmental models,  
501 *Environmental Modelling & Software*, 40, 1–20, <https://doi.org/10.1016/j.envsoft.2012.09.011>, 2013.
- 502 Bérard, P.: Alimentation en eau de la ville de Montpellier: captage de la source du Lez—étude des  
503 relations entre la source et son réservoir aquifère [Water supply of Montpellier: Lez Spring catchment—  
504 study of the relationship between the spring and its aquifer], BRGM, Montpellier, France, 1983.
- 505 Bergström, S.: The HBV model - its structure and applications., 1992.
- 506 Beven, K.: On explanatory depth and predictive power, *Hydrological Processes*, 15, 3069–3072,  
507 <https://doi.org/10.1002/hyp.500>, 2001.
- 508 Beven, K.: A manifesto for the equifinality thesis, *Journal of Hydrology*, 320, 18–36,  
509 <https://doi.org/10.1016/j.jhydrol.2005.07.007>, 2006.
- 510 Bittner, D., Narany, T. S., Kohl, B., Disse, M., and Chiogna, G.: Modeling the hydrological impact of  
511 land use change in a dolomite-dominated karst system, *Journal of Hydrology*, 567, 267–279,  
512 <https://doi.org/10.1016/j.jhydrol.2018.10.017>, 2018.
- 513 Bittner, D., Richieri, B., and Chiogna, G.: Unraveling the time-dependent relevance of input model  
514 uncertainties for a lumped hydrologic model of a pre-alpine karst system, *Hydrogeol J*,  
515 <https://doi.org/10.1007/s10040-021-02377-1>, 2021.
- 516 Blöschl, G., Bierkens, M. F. P., Chambel, A., Cudennec, C., Destouni, G., Fiori, A., Kirchner, J. W.,  
517 McDonnell, J. J., Savenije, H. H. G., Sivapalan, M., Stumpp, C., Toth, E., Volpi, E., Carr, G., Lupton,  
518 C., Salinas, J., Széles, B., Viglione, A., Aksoy, H., Allen, S. T., Amin, A., Andréassian, V., Arheimer,  
519 B., Aryal, S. K., Baker, V., Bardsley, E., Barendrecht, M. H., Bartosova, A., Batelaan, O., Berghuijs,

520 W. R., Beven, K., Blume, T., Bogaard, T., Borges de Amorim, P., Böttcher, M. E., Boulet, G., Breinl,  
521 K., Brilly, M., Brocca, L., Buytaert, W., Castellarin, A., Castelletti, A., Chen, X., Chen, Y., Chen, Y.,  
522 Chiffard, P., Claps, P., Clark, M. P., Collins, A. L., Croke, B., Dathe, A., David, P. C., de Barros, F. P.  
523 J., de Rooij, G., Di Baldassarre, G., Driscoll, J. M., Duethmann, D., Dwivedi, R., Eris, E., Farmer, W.  
524 H., Feiccabrino, J., Ferguson, G., Ferrari, E., Ferraris, S., Fersch, B., Finger, D., Foglia, L., Fowler, K.,  
525 Gartsman, B., Gascoin, S., Gaume, E., Gelfan, A., Geris, J., Gharari, S., Gleeson, T., Glendell, M.,  
526 Gonzalez Bevacqua, A., González-Dugo, M. P., Grimaldi, S., Gupta, A. B., Guse, B., Han, D., Hannah,  
527 D., Harpold, A., Haun, S., Heal, K., Helfricht, K., Herrnegger, M., Hipsey, M., Hlaváčiková, H.,  
528 Hohmann, C., Holko, L., Hopkinson, C., Hrachowitz, M., Illangasekare, T. H., Inam, A., Innocente, C.,  
529 Istanbuloglu, E., Jarihani, B., et al.: Twenty-three unsolved problems in hydrology (UPH) – a  
530 community perspective, *Hydrological Sciences Journal*, 64, 1141–1158,  
531 <https://doi.org/10.1080/02626667.2019.1620507>, 2019.

532 Çallı, S. S., Çallı, K. Ö., Tuğrul Yılmaz, M., and Çelik, M.: Contribution of the satellite-data driven  
533 snow routine to a karst hydrological model, *Journal of Hydrology*, 607, 127511,  
534 <https://doi.org/10.1016/j.jhydrol.2022.127511>, 2022.

535 Chang, Y., Hartmann, A., Liu, L., Jiang, G., and Wu, J.: Identifying More Realistic Model Structures  
536 by Electrical Conductivity Observations of the Karst Spring, *Water Resources Research*, 57,  
537 e2020WR028587, <https://doi.org/10.1029/2020WR028587>, 2021.

538 Chen, Z. and Goldscheider, N.: Modeling spatially and temporally varied hydraulic behavior of a folded  
539 karst system with dominant conduit drainage at catchment scale, Hochifen–Gottesacker, Alps, *Journal*  
540 *of Hydrology*, 514, 41–52, <https://doi.org/10.1016/j.jhydrol.2014.04.005>, 2014.

541 Chen, Z., Hartmann, A., Wagener, T., and Goldscheider, N.: Dynamics of water fluxes and storages in  
542 an Alpine karst catchment under current and potential future climate conditions, *Hydrology and Earth*  
543 *System Sciences*, 22, 3807–3823, <https://doi.org/10.5194/hess-22-3807-2018>, 2018.

544 Cinkus, G., Wunsch, A., Mazzilli, N., Liesch, T., Chen, Z., Ravbar, N., Doummar, J., Fernández-Ortega,  
545 J., Barberá, J. A., Andreo, B., Goldscheider, N., and Jourde, H.: Comparison of artificial neural networks  
546 and reservoir models for simulating karst spring discharge on five test sites in the Alpine and  
547 Mediterranean regions, *Hydrology and Earth System Sciences*, 27, 1961–1985,  
548 <https://doi.org/10.5194/hess-27-1961-2023>, 2023a.

549 Cinkus, G., Mazzilli, N., Jourde, H., Wunsch, A., Liesch, T., Ravbar, N., Chen, Z., and Goldscheider,  
550 N.: When best is the enemy of good – critical evaluation of performance criteria in hydrological models,  
551 *Hydrology and Earth System Sciences*, 27, 2397–2411, <https://doi.org/10.5194/hess-27-2397-2023>,  
552 2023b.

553 Clauzon, V., Mayolle, S., Leonardi, V., Brunet, P., Soliva, R., Marchand, P., Massonnat, G., Rolando,  
554 J.-P., and Pistre, S.: Fault zones in limestones: impact on karstogenesis and groundwater flow (Lez  
555 aquifer, southern France), *Hydrogeol J*, <https://doi.org/10.1007/s10040-020-02189-9>, 2020.

556 Cos, J., Doblas-Reyes, F., Jury, M., Marcos, R., Bretonnière, P.-A., and Samsó, M.: The Mediterranean  
557 climate change hotspot in the CMIP5 and CMIP6 projections, *Earth System Dynamics*, 13, 321–340,  
558 <https://doi.org/10.5194/esd-13-321-2022>, 2022.

559 Cousquer, Y. and Jourde, H.: Reducing Uncertainty of Karst Aquifer Modeling with Complementary  
560 Hydrological Observations for the Sustainable Management of Groundwater Resources, *Journal of*  
561 *Hydrology*, 128130, <https://doi.org/10.1016/j.jhydrol.2022.128130>, 2022.

562 Cousquer, Y., Sivelles, V., and Jourde, H.: Estimating the Structural Uncertainty of Lumped Parameter  
563 Models in Karst Hydrology: a Bayesian Model Averaging (BMA), *Copernicus Meetings*, 2022.

564 Criss, R. E. and Winston, W. E.: Do Nash values have value? Discussion and alternate proposals,  
565 *Hydrological Processes*, 22, 2723–2725, <https://doi.org/10.1002/hyp.7072>, 2008.

566 Dakhlaoui, H. and Djebbi, K.: Evaluating the impact of rainfall–runoff model structural uncertainty on  
567 the hydrological rating of regional climate model simulations, *Journal of Water and Climate Change*,  
568 12, 3820–3838, <https://doi.org/10.2166/wcc.2021.004>, 2021.

569 Darbandsari, P. and Coulibaly, P.: Inter-comparison of lumped hydrological models in data-scarce  
570 watersheds using different precipitation forcing data sets: Case study of Northern Ontario, Canada,  
571 *Journal of Hydrology: Regional Studies*, 31, 100730, <https://doi.org/10.1016/j.ejrh.2020.100730>, 2020.

572 Diffenbaugh, N. S. and Giorgi, F.: Climate change hotspots in the CMIP5 global climate model  
573 ensemble, *Climatic Change*, 114, 813–822, <https://doi.org/10.1007/s10584-012-0570-x>, 2012.

574 Doummar, J., Sauter, M., and Geyer, T.: Simulation of flow processes in a large scale karst system with  
575 an integrated catchment model (Mike She) – Identification of relevant parameters influencing spring  
576 discharge, *Journal of Hydrology*, 426–427, 112–123, <https://doi.org/10.1016/j.jhydrol.2012.01.021>,  
577 2012.

578 Doummar, J., Hassan Kassem, A., and Gurdak, J. J.: Impact of historic and future climate on spring  
579 recharge and discharge based on an integrated numerical modelling approach: Application on a snow-  
580 governed semi-arid karst catchment area, *Journal of Hydrology*, 565, 636–649,  
581 <https://doi.org/10.1016/j.jhydrol.2018.08.062>, 2018.

582 Dubois, E., Doummar, J., Pistre, S., and Larocque, M.: Calibration of a lumped karst system model and  
583 application to the Qachqouch karst spring (Lebanon) under climate change conditions, *Hydrology and*  
584 *Earth System Sciences*, 24, 4275–4290, <https://doi.org/10.5194/hess-24-4275-2020>, 2020.

585 Duran, L., Massei, N., Lecoq, N., Fournier, M., and Labat, D.: Analyzing multi-scale hydrodynamic  
586 processes in karst with a coupled conceptual modeling and signal decomposition approach, *Journal of*  
587 *Hydrology*, 583, 124625, <https://doi.org/10.1016/j.jhydrol.2020.124625>, 2020.

588 Ebel, B. A. and Loague, K.: Physics-based hydrologic-response simulation: Seeing through the fog of  
589 equifinality, *Hydrological Processes*, 20, 2887–2900, <https://doi.org/10.1002/hyp.6388>, 2006.

590 Eberhart, R. and Kennedy, J.: Particle swarm optimization, in: *Proceedings of the IEEE international*  
591 *conference on neural networks*, 1942–1948, 1995.

592 Elshall, A. S., Arik, A. D., El-Kadi, A. I., Pierce, S., Ye, M., Burnett, K. M., Wada, C. A., Bremer, L.  
593 L., and Chun, G.: Groundwater sustainability: a review of the interactions between science and policy,  
594 *Environ. Res. Lett.*, 15, 093004, <https://doi.org/10.1088/1748-9326/ab8e8c>, 2020.

595 Ferreira, P. M. de L., Paz, A. R. da, and Bravo, J. M.: Objective functions used as performance metrics  
596 for hydrological models: state-of-the-art and critical analysis, *RBRH*, 25, e42,  
597 <https://doi.org/10.1590/2318-0331.252020190155>, 2020.

598 Ficchi, A., Perrin, C., and Andréassian, V.: Impact of temporal resolution of inputs on hydrological  
599 model performance: An analysis based on 2400 flood events, *Journal of Hydrology*, 538, 454–470,  
600 <https://doi.org/10.1016/j.jhydrol.2016.04.016>, 2016.

601 Fiorillo, F., Leone, G., Pagnozzi, M., and Esposito, L.: Long-term trends in karst spring discharge and  
602 relation to climate factors and changes, *Hydrogeol J*, 29, 347–377, [https://doi.org/10.1007/s10040-020-](https://doi.org/10.1007/s10040-020-02265-0)  
603 [02265-0](https://doi.org/10.1007/s10040-020-02265-0), 2021.

604 Fleury, P., Plagnes, V., and Bakalowicz, M.: Modelling of the functioning of karst aquifers with a  
605 reservoir model: Application to Fontaine de Vaucluse (South of France), *Journal of Hydrology*, 345,  
606 38–49, <https://doi.org/10.1016/j.jhydrol.2007.07.014>, 2007.

607 Fleury, P., Ladouche, B., Conroux, Y., Jourde, H., and Dörfliger, N.: Modelling the hydrologic functions  
608 of a karst aquifer under active water management – The Lez spring, *Journal of Hydrology*, 365, 235–  
609 243, <https://doi.org/10.1016/j.jhydrol.2008.11.037>, 2009.

610 Ford, D. and Williams, P.: *Karst hydrogeology and geomorphology*, John Wiley & Sons, Hoboken, NJ,  
611 USA, 2013.

612 Frank, S., Goeppert, N., and Goldscheider, N.: Improved understanding of dynamic water and mass  
613 budgets of high-alpine karst systems obtained from studying a well-defined catchment area,  
614 *Hydrological Processes*, 35, e14033, <https://doi.org/10.1002/hyp.14033>, 2021.

615 Freedman, D., Pisani, R., Purves, R., and Adhikari, A.: *Statistics*, WW Norton & Company New York,  
616 2007.

617 Guinot, V., Savéan, M., Jourde, H., and Neppel, L.: Conceptual rainfall–runoff model with a two-  
618 parameter, infinite characteristic time transfer function, *Hydrological Processes*, 29, 4756–4778,  
619 <https://doi.org/10.1002/hyp.10523>, 2015.

620 Gupta, A. and Govindaraju, R. S.: Propagation of structural uncertainty in watershed hydrologic models,  
621 *Journal of Hydrology*, 575, 66–81, <https://doi.org/10.1016/j.jhydrol.2019.05.026>, 2019.

622 Gupta, H. V., Kling, H., Yilmaz, K. K., and Martinez, G. F.: Decomposition of the mean squared error  
623 and NSE performance criteria: Implications for improving hydrological modelling, *Journal of*  
624 *Hydrology*, 377, 80–91, <https://doi.org/10.1016/j.jhydrol.2009.08.003>, 2009.

625 Hartmann, A., Lange, J., Vivó Aguado, À., Mizyed, N., Smiatek, G., and Kunstmann, H.: A multi-model  
626 approach for improved simulations of future water availability at a large Eastern Mediterranean karst  
627 spring, *Journal of Hydrology*, 468–469, 130–138, <https://doi.org/10.1016/j.jhydrol.2012.08.024>, 2012.

628 Hartmann, A., Wagener, T., Rimmer, A., Lange, J., Brielmann, H., and Weiler, M.: Testing the realism  
629 of model structures to identify karst system processes using water quality and quantity signatures, *Water*  
630 *Resour. Res.*, 49, 3345–3358, <https://doi.org/10.1002/wrcr.20229>, 2013.

631 Hauduc, H., Neumann, M. B., Muschalla, D., Gamerith, V., Gillot, S., and Vanrolleghem, P. A.:  
632 Efficiency criteria for environmental model quality assessment: A review and its application to  
633 wastewater treatment, *Environmental Modelling & Software*, 68, 196–204,  
634 <https://doi.org/10.1016/j.envsoft.2015.02.004>, 2015.

635 Jackson, E. K., Roberts, W., Nelsen, B., Williams, G. P., Nelson, E. J., and Ames, D. P.: Introductory  
636 overview: Error metrics for hydrologic modelling – A review of common practices and an open source  
637 library to facilitate use and adoption, *Environmental Modelling & Software*, 119, 32–48,  
638 <https://doi.org/10.1016/j.envsoft.2019.05.001>, 2019.

639 Jeannin, P.-Y., Artigue, G., Butscher, C., Chang, Y., Charlier, J.-B., Duran, L., Gill, L., Hartmann, A.,  
640 Johannet, A., Jourde, H., Kavousi, A., Liesch, T., Liu, Y., Lüthi, M., Malard, A., Mazzilli, N., Pardo-  
641 Igúzquiza, E., Thiéry, D., Reimann, T., Schuler, P., Wöhling, T., and Wunsch, A.: Karst modelling



642 challenge 1: Results of hydrological modelling, *Journal of Hydrology*, 126508,  
643 <https://doi.org/10.1016/j.jhydrol.2021.126508>, 2021.

644 Jiang, T., Chen, Y. D., Xu, C., Chen, X., Chen, X., and Singh, V. P.: Comparison of hydrological impacts  
645 of climate change simulated by six hydrological models in the Dongjiang Basin, South China, *Journal*  
646 *of Hydrology*, 336, 316–333, <https://doi.org/10.1016/j.jhydrol.2007.01.010>, 2007.

647 Jones, R. N., Chiew, F. H. S., Boughton, W. C., and Zhang, L.: Estimating the sensitivity of mean annual  
648 runoff to climate change using selected hydrological models, *Advances in Water Resources*, 29, 1419–  
649 1429, <https://doi.org/10.1016/j.advwatres.2005.11.001>, 2006.

650 Jourde, H., Lafare, A., Mazzilli, N., Belaud, G., Neppel, L., Dörfliger, N., and Cernesson, F.: Flash flood  
651 mitigation as a positive consequence of anthropogenic forcing on the groundwater resource in a karst  
652 catchment, *Environ Earth Sci*, 71, 573–583, <https://doi.org/10.1007/s12665-013-2678-3>, 2014.

653 Klemeš, V.: Operational testing of hydrological simulation models, *Hydrological Sciences Journal*, 31,  
654 13–24, <https://doi.org/10.1080/02626668609491024>, 1986.

655 Knoben, W. J. M., Freer, J. E., Peel, M. C., Fowler, K. J. A., and Woods, R. A.: A Brief Analysis of  
656 Conceptual Model Structure Uncertainty Using 36 Models and 559 Catchments, *Water Resources*  
657 *Research*, 56, e2019WR025975, <https://doi.org/10.1029/2019WR025975>, 2020.

658 Labat, D., Argouze, R., Mazzilli, N., Ollivier, C., and Sivelles, V.: Impact of Withdrawals on Karst  
659 Watershed Water Supply, *Water*, 14, 1339, <https://doi.org/10.3390/w14091339>, 2022.

660 Lee, A.: pyswarm: Particle swarm optimization (PSO) with constraint support, 2014.

661 Liu, Y., Wagener, T., and Hartmann, A.: Assessing Streamflow Sensitivity to Precipitation Variability  
662 in Karst-Influenced Catchments With Unclosed Water Balances, *Water Resources Research*, 57,  
663 e2020WR028598, <https://doi.org/10.1029/2020WR028598>, 2021.

664 Mazzilli, N. and Bertin, D.: KarstMod User Guide - version 2.2, 2019.

665 Mazzilli, N., Guinot, V., and Jourde, H.: Sensitivity analysis of conceptual model calibration to  
666 initialisation bias. Application to karst spring discharge models, *Advances in Water Resources*, 42, 1–  
667 16, <https://doi.org/10.1016/j.advwatres.2012.03.020>, 2012.

668 Mazzilli, N., Guinot, V., Jourde, H., Lecoq, N., Labat, D., Arfib, B., Baudement, C., Danquigny, C., Dal  
669 Soglio, L., and Bertin, D.: KarstMod: A modelling platform for rainfall - discharge analysis and  
670 modelling dedicated to karst systems, *Environmental Modelling & Software*, 122, 103927,  
671 <https://doi.org/10.1016/j.envsoft.2017.03.015>, 2019.

672 Mazzilli, N., Sivelles, V., Cinkus, G., Jourde, H., and Bertin, D.: KarstMod User Guide - version 3.0,  
673 2022.

674 McMillan, H., Jackson, B., Clark, M., Kavetski, D., and Woods, R.: Rainfall uncertainty in hydrological  
675 modelling: An evaluation of multiplicative error models, *Journal of Hydrology*, 400, 83–94,  
676 <https://doi.org/10.1016/j.jhydrol.2011.01.026>, 2011.

677 Moges, E., Demissie, Y., Larsen, L., and Yassin, F.: Review: Sources of Hydrological Model  
678 Uncertainties and Advances in Their Analysis, *Water*, 13, 28, <https://doi.org/10.3390/w13010028>, 2021.

679 Moriasi, D. N., Arnold, J. G., Liew, M. W. V., Bingner, R. L., Harmel, R. D., and Veith, T. L.: Model  
680 Evaluation Guidelines for Systematic Quantification of Accuracy in Watershed Simulations,  
681 *Transactions of the ASABE*, 50, 885–900, <https://doi.org/10.13031/2013.23153>, 2007.

682 Nash, J. E. and Sutcliffe, J. V.: River flow forecasting through conceptual models part I — A discussion  
683 of principles, *Journal of Hydrology*, 10, 282–290, [https://doi.org/10.1016/0022-1694\(70\)90255-6](https://doi.org/10.1016/0022-1694(70)90255-6), 1970.

684 Nerantzaki, S. D. and Nikolaidis, N. P.: The response of three Mediterranean karst springs to drought  
685 and the impact of climate change, *Journal of Hydrology*, 591, 125296,  
686 <https://doi.org/10.1016/j.jhydrol.2020.125296>, 2020.

687 Ollivier, C., Mazzilli, N., Oliosio, A., Chalikakis, K., Carrière, S. D., Danquigny, C., and Emblanch, C.:  
688 Karst recharge-discharge semi distributed model to assess spatial variability of flows, *Science of The*  
689 *Total Environment*, 703, 134368, <https://doi.org/10.1016/j.scitotenv.2019.134368>, 2020.

690 Oudin, L., Hervieu, F., Michel, C., Perrin, C., Andréassian, V., Anctil, F., and Loumagne, C.: Which  
691 potential evapotranspiration input for a lumped rainfall–runoff model? Part 2—Towards a simple and  
692 efficient potential evapotranspiration model for rainfall–runoff modelling, *Journal of Hydrology*, 303,  
693 290–306, <https://doi.org/10.1016/j.jhydrol.2004.08.026>, 2005.

694 Pandi, D., Kothandaraman, S., and Kuppasamy, M.: Hydrological models: a review, *International*  
695 *Journal of Hydrology Science and Technology*, 12, 223–242,  
696 <https://doi.org/10.1504/IJHST.2021.117540>, 2021.

697 Pechlivanidis, I., Jackson, B., McMillan, H., and Gupta, H. V.: Using an informational entropy-based  
698 metric as a diagnostic of flow duration to drive model parameter identification, *Global NEST Journal*,  
699 14, 325–334, <https://doi.org/10.30955/gnj.000879>, 2013.

700 Perrin, C., Michel, C., and Andréassian, V.: Does a large number of parameters enhance model  
701 performance? Comparative assessment of common catchment model structures on 429 catchments,  
702 *Journal of Hydrology*, 242, 275–301, [https://doi.org/10.1016/S0022-1694\(00\)00393-0](https://doi.org/10.1016/S0022-1694(00)00393-0), 2001.

703 Pianosi, F., Sarrazin, F., and Wagener, T.: A Matlab toolbox for Global Sensitivity Analysis,  
704 *Environmental Modelling & Software*, 70, 80–85, <https://doi.org/10.1016/j.envsoft.2015.04.009>, 2015.

705 Pianosi, F., Sarrazin, F., and Wagener, T.: How successfully is open-source research software adopted?  
706 Results and implications of surveying the users of a sensitivity analysis toolbox, *Environmental*  
707 *Modelling & Software*, 124, 104579, <https://doi.org/10.1016/j.envsoft.2019.104579>, 2020.

708 Pool, S., Vis, M., and Seibert, J.: Evaluating model performance: towards a non-parametric variant of  
709 the Kling-Gupta efficiency, *Hydrological Sciences Journal*, 63, 1941–1953,  
710 <https://doi.org/10.1080/02626667.2018.1552002>, 2018.

711 Poulain, A., Watlet, A., Kaufmann, O., Van Camp, M., Jourde, H., Mazzilli, N., Rochez, G., Deleu, R.,  
712 Quinif, Y., and Hallet, V.: Assessment of groundwater recharge processes through karst vadose zone by  
713 cave percolation monitoring, *Hydrological Processes*, 32, 2069–2083,  
714 <https://doi.org/10.1002/hyp.13138>, 2018.

715 Sarrazin, F., Hartmann, A., Pianosi, F., Rosolem, R., and Wagener, T.: V2Karst V1.1: a parsimonious  
716 large-scale integrated vegetation–recharge model to simulate the impact of climate and land cover  
717 change in karst regions, *Geosci. Model Dev.*, 11, 4933–4964, [https://doi.org/10.5194/gmd-11-4933-](https://doi.org/10.5194/gmd-11-4933-2018)  
718 2018, 2018.

719 Schwemmler, R., Demand, D., and Weiler, M.: Technical note: Diagnostic efficiency – specific  
720 evaluation of model performance, *Hydrology and Earth System Sciences*, 25, 2187–2198,  
721 <https://doi.org/10.5194/hess-25-2187-2021>, 2021.

722 Shmueli, G.: To Explain or to Predict?, *Statistical Science*, 25, 289–310, [https://doi.org/10.1214/10-](https://doi.org/10.1214/10-STS330)  
723 STS330, 2010.

724 Sivellev, V. and Jourde, H.: A methodology for the assessment of groundwater resource variability in  
725 karst catchments with sparse temporal measurements, *Hydrogeol J*, 29, 137–157,  
726 <https://doi.org/10.1007/s10040-020-02239-2>, 2020.

727 Sivellev, V., Labat, D., Mazzilli, N., Massei, N., and Jourde, H.: Dynamics of the Flow Exchanges  
728 between Matrix and Conduits in Karstified Watersheds at Multiple Temporal Scales, *Water*, 11, 569,  
729 <https://doi.org/10.3390/w11030569>, 2019.

730 Sivelles, V., Jourde, H., Bittner, D., Mazzilli, N., and Trambly, Y.: Assessment of the relative impacts  
731 of climate changes and anthropogenic forcing on spring discharge of a Mediterranean karst system,  
732 *Journal of Hydrology*, 598, 126396, <https://doi.org/10.1016/j.jhydrol.2021.126396>, 2021.

733 Sivelles, V., Pérotin, L., Ladouche, B., de Montety, V., Bailly-Comte, V., Champollion, C., and Jourde,  
734 H.: A lumped parameter model to evaluate the relevance of excess air as a tracer of exchanged flows  
735 between transmissive and capacitive compartments of karst systems, *Frontiers in Water*, 4, 2022a.

736 Sivelles, V., Jourde, H., Bittner, D., Richieri, B., Labat, D., Hartmann, A., and Chiogna, G.: Considering  
737 land cover and land use (LCLU) in lumped parameter modeling in forest dominated karst catchments,  
738 *Journal of Hydrology*, 612, 128264, <https://doi.org/10.1016/j.jhydrol.2022.128264>, 2022b.

739 Smiatek, G., Kaspar, S., and Kunstmann, H.: Hydrological Climate Change Impact Analysis for the  
740 Fiegh Spring near Damascus, Syria, *Journal of Hydrometeorology*, 14, 577–593,  
741 <https://doi.org/10.1175/JHM-D-12-065.1>, 2013.

742 Sobol, I. M.: On quasi-Monte Carlo integrations, *Mathematics and Computers in Simulation*, 47, 103–  
743 112, [https://doi.org/10.1016/S0378-4754\(98\)00096-2](https://doi.org/10.1016/S0378-4754(98)00096-2), 1998.

744 Sophocleous, M.: Interactions between groundwater and surface water: the state of the science,  
745 *Hydrogeology Journal*, 10, 52–67, <https://doi.org/10.1007/s10040-001-0170-8>, 2002.

746 Stevanović, Z.: Karst waters in potable water supply: a global scale overview, *Environ Earth Sci*, 78,  
747 662, <https://doi.org/10.1007/s12665-019-8670-9>, 2019.

748 Westerberg, I. K., Sikorska-Senoner, A. E., Viviroli, D., Vis, M., and Seibert, J.: Hydrological model  
749 calibration with uncertain discharge data, *Hydrological Sciences Journal*, 0, null,  
750 <https://doi.org/10.1080/02626667.2020.1735638>, 2020.

751 Zhou, S., Wang, Y., Li, Z., Chang, J., and Guo, A.: Quantifying the Uncertainty Interaction Between  
752 the Model Input and Structure on Hydrological Processes, *Water Resour Manage*, 35, 3915–3935,  
753 <https://doi.org/10.1007/s11269-021-02883-7>, 2021.

754